Computational Permeability Sensitivity of Parachutes

Rishabh Srinivas * and Cutler Phillippe
The Grainger College of Engineering, Aerospace Engineering at University of Illinois Urbana-Champaign, Urbana Illinois, 61801

This study investigates the sensitivity of parachute drag to textile porosity, focusing on effective (c_e) and geometric porosity (γ_g). The study identified critical variables that affect the drag coefficient (C_D) under different conditions using equations derived from fluid dynamics and sensitivity analysis tools such as Sobol indices. The results highlight the dominance of the discharge coefficient (k) and porosity-related factors in determining parachute performance, with material deformation and Reynolds per unit length ($\hat{R}e$) further refining the analysis. The findings offer a predictive framework for parachute optimization, improving design strategies for diverse applications.

Nomenclature

c_e = effective porosity [dimensionless]

V = 'fictitious velocity' from Δp $[m/s]$

u = velocity through material $[m/s]$

Δp = pressure differential (what units are here?)

ρ = density$[kg/m^3]$

k_1 = pressure loss related constant [dimensionless]

k_2 = viscous loss related constant $[m^-1]$

μ = dynamic viscosity(what units are here?)

$\hat{R}e$ = Reynolds per unit length (what units are here?)

λ_T = total porosity [dimensionless]

γ_g = geometric porosity [dimensionless]

k = discharge coefficient [dimensionless]

D = drag $[N]$

S_p = parachute projected area $[m^2]$

C_D = drag coefficient [dimensionless]

*Undergraduate Student, Aerospace Engineering Department, 918 W Illinois St, Urbana, IL 61801 0237B, and AIAA Student Member.

I. Introduction

Parachutes play a crucial role in various industries, including aerospace, military, and rescue operations, by controlling the descent velocity. Additionally, parachutes ensure safety during the entry, descent, and landing (EDL) phase for space exploration[1].

Parachutes lower the terminal velocity, the maximum speed of descent, by increasing the opposing force by trapping air under the parachute textile. This opposing force, known as drag, acts in the opposite direction of gravity during descent. The drag force is calculated using the fundamental fluid dynamics equation:

$$F_d = \frac{1}{2} * \rho * v^2 * C_d * A$$

In this equation, the drag force (F_d) is directly proportional to the drag coefficient (C_d), air density (ρ), velocity (v), and cross-sectional area (A). This equation shows that the drag coefficient is directly proportional to the drag force acting on the parachute; increasing the drag coefficient raises the drag force, which reduces the time taken to reach terminal velocity and, consequently, lowers the terminal velocity.

Parachute performance is highly dependent on the textile's properties and the parachute's design. The microstructure of the textile, especially its porosity, plays a significant role. As noted by Heinrich, "If the parachute cloth is considered to be a screen through which, during the use of the parachute, a certain amount of air passes, one may assume that the air permeability or porosity of this screen depends on the Reynolds and Mach numbers of the flow conditions.[2]" The Reynolds number (Re) is a dimensionless quantity in fluid mechanics that predicts flow patterns by representing the ratio of inertial forces to viscous forces within a fluid. The Mach number defines the ratio of local flow velocity to the local speed of sound in the same fluid, quantifying the degree of compressibility effects in a flow[3].

The microstructure of parachutes refers to the arrangement and composition of the fibers in the textile, including factors such as fiber density, weave pattern, and porosity. Controlling these factors directly impacts the effectiveness of parachutes.

Strain occurs when the parachute textile is subjected to pressures causing deformation in its physical structure. This strain manifests as stretching, compression, or bending of the fibers, altering the geometry of the fabric. Over time, these changes reduce the parachute's performance by affecting its air permeability and flexibility. For instance, the ability of the textile to generate drag diminishes as the material stretches and becomes more porous, allowing more air to pass through rather than trapping it. Additionally, fluctuations in pressure during deployment and descent may exacerbate material fatigue, contributing to changes in the fibers that weakens the overall integrity[4].

The main goal is to conduct a sensitivity drag coefficient to determine the total porosity and the coefficient of drag given various factors, allowing for the substitution of real values. Sensitivity analysis provides users of mathematical and simulation models with tools to appreciate the dependency of the model output on the model input, enabling

investigation into the importance of each input.

II. Schedule

This project was carried out during the Fall 2024 semester. I met regularly with my mentor for about two hours weekly to discuss project progress, next steps, knowledge confirmation, and possible future project directions.

III. Theory

Firstly, the definition of effective porosity is given by Heinrich he found while passing air through different cloth samples is defined as the ratio of the measured velocity to the ideal flow velocity[2]:

$$c_e = \frac{u}{V} \tag{1}$$

This equation is derived from the fundamental dynamic pressure equation because the pressure differential is important for estimating parachute drag coefficients[2]:

$$\Delta p = \frac{1}{2}\rho V^2 \quad \Longrightarrow \quad V = \sqrt{\frac{2\Delta p}{\rho}} \tag{2}$$

In this equation, the pressure differential (or the dynamic pressure) is directly proportional to the fluid density and the square of the fictitious velocity from Δp. For simplicity in further derivations, fictitious velocity is solved as shown above. Another format to solve for the pressure differential is the following equation where k_1 is a dimensionless constant based on the momentum equation and k_2 is a non-dimensionless constant that comes from the Hagen-Poiseulle flow case assuming pores are laminar flow channels thus k_2 absorbs other terms that are not μ and u. Essentially, the following equation is a summation of pressure loss terms converted into a two-constant form to allow material parameter fitting[3, 4]:

$$\Delta p = k_1 \rho u^2 + k_2 \mu u \tag{3}$$

In this equation (the first part) is the pressure loss and the (second part) is the viscous loss. Then the velocity through the material is solved for leading to the following equation[5]:

$$u = \frac{-k_2\mu}{2k_1\rho} + \sqrt{\frac{\Delta p}{k_1\rho} + \left(\frac{k_2 u}{2k_1\rho}\right)^2} \tag{4}$$

Given the Reynolds per unit length formula and the new definition for fictitious velocity, the following equation is given:

$$R\hat{e} = \frac{\rho V}{\mu} = \frac{\sqrt{2\Delta p \rho}}{\mu} \tag{5}$$

Substituting the equations for velocity through the material and the 'fictitious' velocity into Heinrich's initial equation (1), Lingard states effective porosity written as a function of k_1, k_2, and the new definition of the Reynolds per unit length formula (5)[5].

$$c_e = \frac{-k_2}{2k_1 R\hat{e}} + \sqrt{\frac{1}{2k_1} + \left(\frac{k_2}{2k_1 R\hat{e}}\right)^2} \tag{6}$$

Lingard first developed a concrete equation for total porosity by assuming perfect discharge and not allowing for open areas in the material, Cruz then updated this equation to fit better after testing[5, 6].

$$\lambda_T = \gamma_g + c_e \quad \Longrightarrow \quad \lambda_T = k\gamma_g + \left(1 - \gamma_g\right) c_e \tag{7}$$

Then the new definition for effective porosity (6), is substituted to create the following equation[6] :

$$\lambda_T = k\gamma_g + \left(1 - \gamma_g\right)\left(\frac{-k_2}{2k_1 R\hat{e}} + \sqrt{\frac{1}{2k_1} + \left(\frac{k_2}{2k_1 R\hat{e}}\right)^2}\right) \tag{8}$$

The Reynolds per unit length must be manipulated to make the equation for total porosity relate to drag. The following equations for drag is used in the Reynolds per unit length equation derived above (5). Then, it can be further manipulated to solve for the pressure differential[5].

$$D = \Delta p S_p \quad \Longrightarrow \quad \Delta p = \frac{D}{S_p} \quad \Longrightarrow \quad R\hat{e} = \frac{\sqrt{\frac{2\rho D}{S_p}}}{\mu} = \sqrt{\frac{2\rho D}{S_p \mu^2}} \tag{9}$$

The new definition for the Reynolds per unit length formula (9) is substituted into the previous equation for total porosity (8) to get the following equation to put total porosity not in terms of the Reynolds unit length but instead controllable and measurable variables.

$$\lambda_T = k\gamma_g + (1 - \gamma_g)\left(\frac{-k_2\mu}{2k_1\sqrt{\frac{2\rho D}{S_p}}} + \sqrt{\frac{1}{2k_1} + \frac{(k_2\mu)^2}{\frac{8k_1^2\rho D}{S_p}}}\right) \tag{10}$$

The coefficient of drag equation from Cruz utilizes this number as well with two constants C_0 and C_1 because they assume the same shape and construction of parachute for different materials, thus giving a different total porosity. They write the coefficient of drag equation to be only based on the total porosity and constants that are specific to the construction of the parachute regardless of the material used[6]:

$$C_D = C_0 + C_1 \lambda_T \tag{11}$$

The total porosity is then substituted into this equation to give the drag coefficient for several other variables.

$$C_D = C_0 + C_1 \left[k\gamma_g + (1-\gamma_g) \left(\frac{-k_2 \mu}{2k_1 \sqrt{\frac{2\rho D}{S_p}}} + \sqrt{\frac{1}{2k_1} + \frac{(k_2\mu)^2}{\frac{8k_1^2 \rho D}{S_p}}} \right) \right] \tag{12}$$

Furthering analysis, Reynolds per unit length can be substituted into the equation to give a better estimate of the true impact of the dimensional variables in their totality.

$$C_D = C_0 + C_1 \left[k\gamma_g + \left(1-\gamma_g\right) \left(\frac{-k_2}{2k_1 R\hat{e}} + \sqrt{\frac{1}{2k_1} + \left(\frac{k_2}{2k_1 R\hat{e}} \right)^2} \right) \right] \tag{13}$$

IV. Methods

To perform the sensitivity analysis, Jupyter Notebook is utilized as the main testing environment for Python, and the following packages are attached: Numpy, Matplotlib, and Scipy. NumPy is a Python library used for numerical computing, offering support for large, multi-dimensional arrays and matrices, along with a wide variety of mathematical functions to operate on these arrays efficiently. Matplotlib is a Python library used for creating static, interactive, and animated visualizations, providing functions to generate plots, charts, and graphs from data. SciPy is a Python library built on NumPy that provides advanced scientific and technical computing tools, including optimization, integration, interpolation, and statistical analysis modules.

Finding the first and total order Sobol indices was the primary method for performing statistical analysis for equations in this context. "The first-order Sobol' index S_j, also denoted by S_j , measures the main effect of the group of inputs $X_j \in \mathbb{R}^{k_j}$ .The first-order Sobol index (denoted as S_i) measures the direct contribution of an individual input variable X_i to the variance of the output"[7], ignoring interactions with other variables. They quantify how much the variability in the output is explained by varying that particular input variable alone. A higher first-order Sobol index indicates that the variable significantly impacts the output by itself. "The total Sobol' index S_j^{tot} measures the effect due to X_j and its interactions with all the other X_k."[7] This index tells the overall importance of a variable in influencing the output, including both its effect and any interaction effects with other variables. These two Sobol Indices also are dependent on the type of distribution of the input variable in their respective bounds. For example, a variable will have a different (first or total) Sobol indices value between using a random distribution or a normal distribution over a given range of the particular variable.

Using Scipy, analysis for these Sobol indices is run easily and numerous times to provide precise data. Using

Matplotlib, the data is then plotted to visually represent Sobol indices and their variation in the form of a dot plot with error bars.

The two equations sensitivity analysis are run for are (7) and (12).

The first equation is a control to determine whether or not the Sobol indices were revealing the correct information based on past knowledge. The three variables analysis is done on k, γ_g, and c_e with respective bounds of [0,1.5], [0,1], and [0,1]. The analysis was over 16,384(2^{14}) points because the SciPy sobol indicies package must use an exponential of 2 for the number of data points.

The second equation analysis is done to determine whether or not any of the variables impact the drag coefficient. the variables analysis is done on are k, γ_g, ρ, D/S_p, and μ with respective bounds of $[0, 1.5]$, $[0, 1]$, $[0.02, 1.8]$, $[1, 7000]$, and $[1 * 10^{-5}, 2 * 10^{-5}$ over 16384 points. D/S_p was used as a single variable to determine the total impact of the three variables that make it up. In addition to finding data from Equation 12, Equation 13 is also used to determine the total impact of the dimensionalized variables.

Determining the Boundaries for the variables were found as follows: for the flow-related ones, they were based on the range of atmospheric properties from Earth, Mars, and Titan. For the material ones, they're ranges that fully encompass both real measured values and any hypothetical values. It should be noted that the range goes far beyond any measured values, and it's expected that the distributions of experimental datasets that will eventually be used in this system of equations will be much narrower.

Table 1 provides experimental values for C_0 and C_1 from Cutler Phillippe. C_0 and C_1 come from wind tunnel data of two parachutes of two textiles, 44370 T.II and 7020 T.III. Multiple pairs of C_0 and C_1 are used to determine whether they have any effect on the Sobol indices of the other variables.

Textiles 44370 T.II and 7020 T.III are used for their different porosity and permeability properties.The permeability specification is 100–160 CFM for 7020 T.III [8] and 30–50 CFM for 44378 T.II[9] Both textiles are constructed using warp tows, longitudinal fibers running parallel to the fabric's length, distributed in a pattern of short and long intertows, connecting fibers between the warp tows that provide structural integrity. Both textiles also feature evenly distributed weft tows, which are the transverse fibers running perpendicular to the warp tows, contribute to the fabric's stability y.However, the spacing in the 44378 T.II textile is less than that of the 7020 T.III textile. A key difference between the Textiles is the pore sizes because 44378 T.II has small pores, with characteristic pore widths between 1 and 10 μm, while 7020 T.III has larger pores, between 10 to 100 μm. The stark difference between textiles makes determining the impact of other variables easier[10]

V. Results

The first-order Sobol indices for Equation 7 in Figure 1 are as follows: 0.49086421, 0.05453075, and 0.21812235 for k, γ_g, c_e respectively. The total order Sobol indices for Equation 7 are as follows: 0.65454586, 0.29091005, and

Table 1 Pairs of C_0 and C_1 values from experimental data

	Constants	
Pair	C_0	C_1
1	0.723598914	-0.102868224
2	0.768239429	-0.484686812
3	0.792003116	-1.082339471
4	0.764404938	-0.938284815

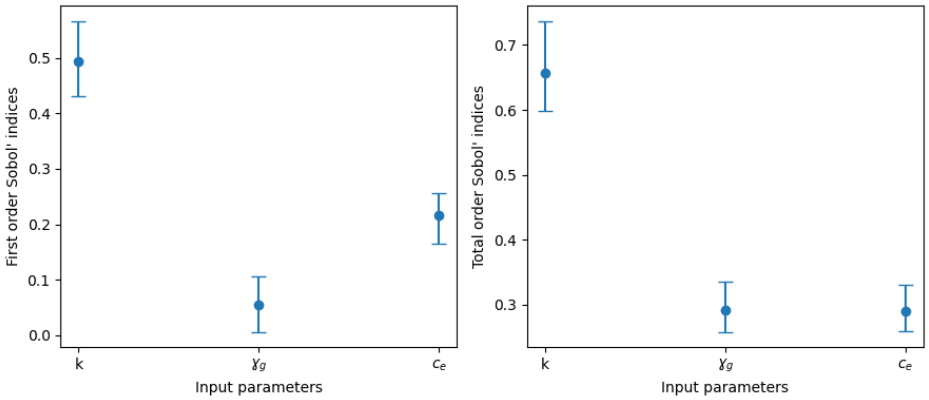

Fig. 1 First and Total Sobol Indices of Equation 7

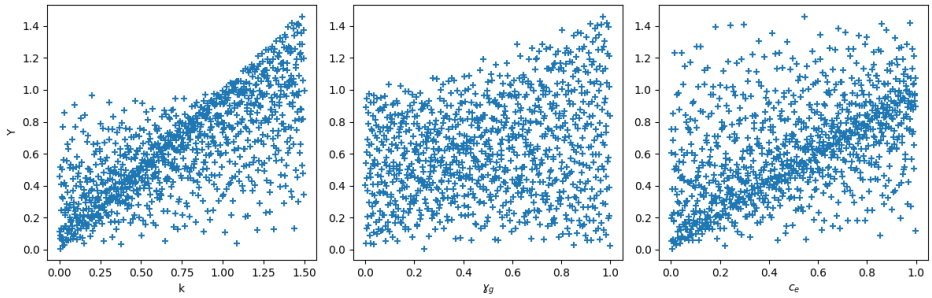

Fig. 2 Distribution of Data within Boundaries For Each Variable in Equation 7

0.29090914 for k, γ_g, and c_e respectively. These values are consistent with the distribution seen in Figure 2 where k is the most linear, followed by c_e and γ_g. Figure 1 also shows the error bars given from the data collection.

The first order Sobol indices for Equation 12 for textile 44370T.II following the seeing in figure 3 are as follows: $9.66159153 * 10^{-3}$, 9.1335973310^{-3}, 1.9070027810^{-5} 1.0007431610^{-4}, -3.0280788610^{-6}, 2.3618280710^{-1}, and 4.3913004210^{-1} for k, γ_g, D/S_p, μ, C_0, and C_1 respectively. The total-order Sobol indices for Equation 7 are as follows: $1.91896253 * 10^{-1}$, $1.81027168 * 10^{-1}$, $1.04675403 * 10^{-5}$, $1.43573793 * 10^{-5}$, $1.58634729e * 10^{-6}$, $2.36147862e * 10^{-1}$, and $7.47381556 * 10^{-1}$ for k, γ_g, D/S_p, μ, C_0, and C_1 respectively. Figure 3 also depicts the error bars given from the data collection.

The first order Sobol indices for Equation 12 for textile 7020TIII seen in figure 4 are as follows: $7.96363955 *$

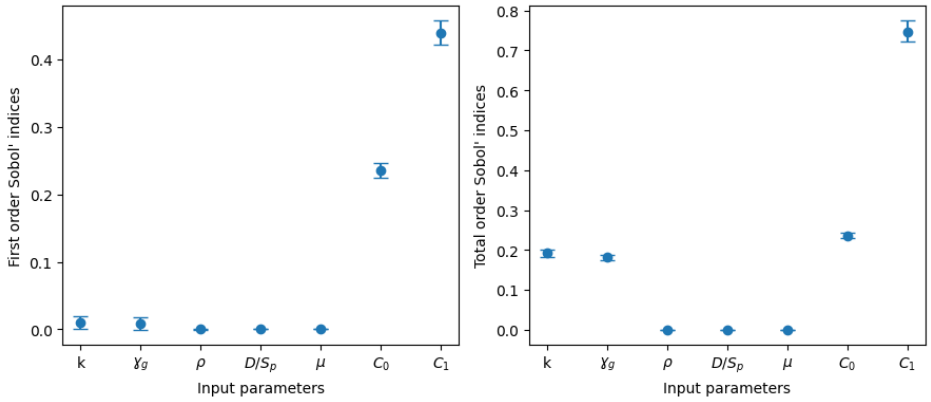

Fig. 3 First and Total Sobol Indices of Equation 12 For Textile 44370TII

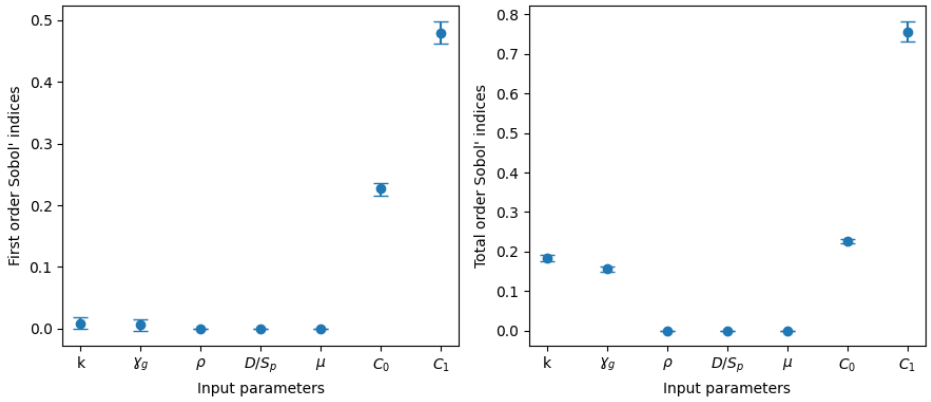

Fig. 4 First and Total Sobol Indices of Equation 12 for textile 7020TIII

10^{-3}, $6.29256285 * 10^{-3}$, $-1.75932074 * 10^{-6}$, $-9.49593574 * 10^{-6}$, $6.48589206 * 10^{-6}$, $2.26734824 * 10^{-1}$, and $4.78803249 * 10^{-1}$ for k, γ_g, D/S_p, μ, C_0, and C_1 respectively. The total order Sobol indices for Equation 7 are as follows: $1.84224946 * 10^{-1}$, $1.56224286 * 10^{-1}$, $1.12860490 * 10^{-5}$, $2.00558819 * 10^{-5}$, $1.48807107 * 10^{-6}$, $2.26737895 * 10^{-1}$, and $7.56337532 * 10^{-1}$ for k, γ_g, D/S_p, μ, C_0, and C_1 respectively. Figure 4 also depicts the error bars given from the data collection.

The first order Sobol indices for Equation 13 for textile 7020TIII seen in figure 5 are as follows: 8.8405804610^{-2}, 8.4031956010^{-2}, 1.5705234910^{-1}, 3.7326274110^{-1}, 5.4376592410^{-5} for k, γ_g, C_0, C_1, and Re respectively. The total order Sobol indices for Equation 7 are as follows: 2.7483794810^{-1}, 2.6374937510^{-1}, 1.5705249110^{-1}, 6.4132229710^{-1}, 1.4801238510^{-4} for k, γ_g, C_0, C_1, and Re respectively. Figure 4 also depicts the error bars given from the data collection.

Table 2 has values for all variables that are comparable to each other.

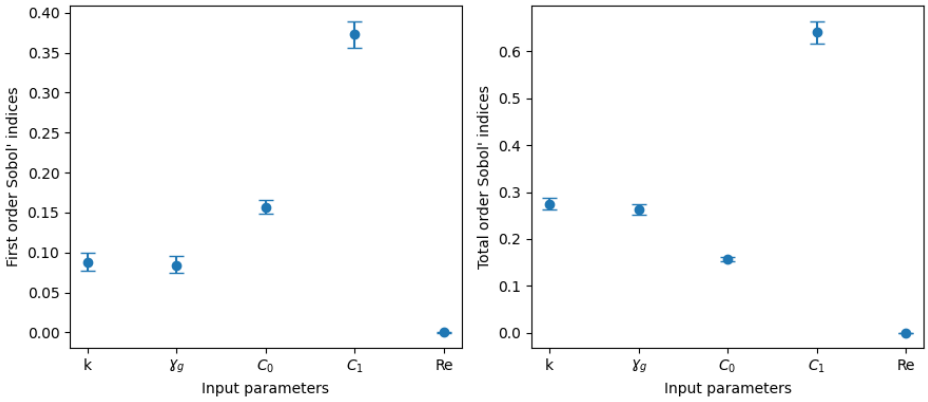

Fig. 5 First and Total Sobol Indices of Equation 13 for textile 7020TIII Using Reynolds Unit

Table 2 First and Total Order Sobol Indices Given Pairs of C_0 and C_1 Constants on Two Textiles

	Pair	Pair 1		Pair 2		Pair 3		Pair 4	
	Material	44378 T.II	7020 T.III	44378 T.II	7020 T.III	44378 T.II	7020 T.III	44378 T.II	7020 T.III
first	k	4.43E-01	4.69E-01	4.43E-01	4.69E-01	4.43E-01	4.69E-01	4.43E-01	4.69E-01
	γ_g	4.09E-01	3.74E-01	4.10E-01	3.74E-01	4.09E-01	3.74E-01	4.09E-01	3.74E-01
	ρ	1.39E-05	3.01E-05	2.94E-05	2.50E-05	2.25E-05	2.74E-05	1.67E-05	4.18E-05
	D/S_p	4.20E-05	6.06E-05	3.13E-05	2.45E-05	1.31E-05	3.06E-05	5.38E-05	6.19E-05
	μ	3.83E-07	-1.98E-06	2.94E-06	7.20E-06	4.92E-06	5.40E-06	3.95E-06	-1.20E-06
total	k	5.91E-01	6.26E-01	5.91E-01	6.26E-01	5.91E-01	6.26E-01	5.91E-01	6.26E-01
	γ_g	5.57E-01	5.31E-01	5.58E-01	5.31E-01	5.57E-01	5.31E-01	5.57E-01	5.31E-01
	ρ	3.20E-05	3.80E-05	3.21E-05	3.80E-05	3.22E-05	3.78E-05	3.21E-05	3.74E-05
	D/S_p	4.44E-05	6.78E-05	4.45E-05	6.82E-05	4.45E-05	6.76E-05	4.44E-05	6.83E-05
	μ	4.83E-06	5.13E-06	4.83E-06	5.21E-06	4.82E-06	5.13E-06	4.83E-06	5.18E-06

VI. Discussion

The sensitivity analysis conducted in this study provides significant insights into the relationship between textile porosity, material properties, and drag coefficients in parachute performance. The findings highlight that the effective porosity (c_e) and geometric porosity (γ_g) are among the most impactful factors influencing total porosity (λ_T) and subsequently the drag coefficient (C_D). This aligns with Heinrich's theory that air permeability depends on Reynolds and Mach numbers under specific flow conditions.

The Sobol indices underscore the importance of the discharge coefficient (k) in determining both first-order and total effects on the drag coefficient, as seen in Figures 1 through 5. Interestingly, the variations in μ (dynamic viscosity) and ρ (fluid mass density) yielded relatively lower Sobol indices, suggesting that while these factors influence the drag, their effects are secondary when compared to porosity-related variables and textile geometry. Moreover, material strain, introduced as a function of porosity evolution over time, was captured indirectly through the variation of λ_T. For textiles 44378TII and 7020TIII, the material constants C_0 and C_1 demonstrated consistent changes in Sobol indices across

different parameter bounds, reflecting their material-specific dependency on λ_T. This observation confirms that minor adjustments in porosity factors significantly alter drag performance.

The introduction of Equation 13, incorporating the Reynolds per unit length (Re), further refined the sensitivity analysis, offering a pathway to dimensionally quantify the dynamic effects of porosity. The high Sobol indices for C_1 in this context emphasize the critical role of this parameter in scaling the drag coefficient based on geometric and flow variables.

VII. Conclusion

This research establishes a comprehensive framework for evaluating the sensitivity of parachute drag performance to its textile properties and material constants. The analysis confirms that porosity, particularly geometric porosity (γ_g) and discharge coefficients (k), significantly dictate the drag characteristics, providing a robust method to predict performance under varying operational conditions.

Future applications of this work include dynamic modeling of parachute textiles subjected to material fatigue or environmental stresses over multiple deployments. Additionally, the refined equations presented serve as a foundation for designing optimized parachutes tailored for specific mission requirements. Ultimately, this study advances our understanding of the complex interplay between textile microstructure and parachute aerodynamic performance.

References

[1] Cruz, J. R., Way, D. W., Shidner, J. D., Davis, J. L., Adams, D. S., and Kipp, D. M., "Reconstruction of the Mars Science Laboratory Parachute Performance," *Journal of Spacecraft and Rockets*, Vol. 51, No. 4, 2014, pp. 1185–1196. https://doi.org/10.2514/1.A32816, URL https://doi.org/10.2514/1.A32816.

[2] Heinrich, H., "THE EFFECTIVE POROSITY OF PARACHUTE CLOTH," 1963, p. 72.

[3] Reynolds, O., *Papers on Mechanical and Physical Subjects: 1881-1900*, Vol. 2, The University Press, 1901.

[4] Payne, P., "The Theory of Fabric Porosity as Applied to Parachutes in Incompressible Flow," *Aeronautical Quarterly*, Vol. 29, 1978, pp. 175–206. https://doi.org/10.1017/S000192590000843X.

[5] Lingard, J., and Underwood, J., "The effects of low density atmospheres on the aerodynamic coefficients of parachutes," 1995. https://doi.org/10.2514/6.1995-1556.

[6] Cruz, J., O'Farrell, C., Hennings, E., and Runnells, P., "Permeability of Two Parachute Fabrics - Measurements, Modeling, and Application," 2017. https://doi.org/10.2514/6.2017-3725.

[7] Prieur, C., Tarantola, S., Ghanem, R., Higdon, D., and Owhadi, H., "Variance-Based Sensitivity Analysis: Theory and

Estimation Algorithms," *Springer International Publishing*, 2017. URL https://link.springer.com/content/pdf/10.1007/978-3-319-12385-1_35.pdf.

[8] "MIL-C-7020 H CLOTH PARACHUTE NYLON-RIP STOP TWILL WEAVE — everyspec.com," http://everyspec.com/MIL-SPECS/MIL-SPECS-MIL-C/MIL-C-7020H_38765/, 1992. [Accessed 12-12-2024].

[9] "MIL-C-44378 CLOTH PARACHUTE NYLON LOW PERMEABILITY — everyspec.com," http://everyspec.com/MIL-SPECS/MIL-SPECS-MIL-C/MIL-C-44378_47035/, 1992. [Accessed 12-12-2024].

[10] Phillippe, C. A., Panerai, F., and Roca, L. V. n., "In Situ Imaging of Parachute Textile Micromechanics Under Tensile Load," *AIAA Journal*, Vol. 62, No. 12, 2024, pp. 4691–4700. https://doi.org/10.2514/1.J064350, URL https://doi.org/10.2514/1.J064350.